ChemComm

COMMUNICATION

View Article Online
View Journal | View Issue

Cite this: *Chem. Commun.*, 2019, **55**, 11924

Received 20th August 2019,
Accepted 9th September 2019

DOI: 10.1039/c9cc06463j

rsc.li/chemcomm

A low-molecular-weight ditopic MRI probe for ratiometric sensing of zwitterionic amino acid neurotransmitters†

Đorđe Toljić and Goran Angelovski *

We report a novel ditopic Gd(III)-based probe selective to zwitterionic amino acid neurotransmitters (ZNTs) crafted for ratiometric MRI imaging. The probe displayed increased binding affinity to ZNTs and non-synchronized concentration-dependent changes of the r_1- and r_2-relaxivity. Through the application of a T_2/T_1 weighted MRI strategy, we demonstrated signal enhancement for cooperatively bound glutamate and γ-aminobutyric acid ZNTs over competitive hydrogencarbonate, which remained MR silent.

A wide variety of neuronal diseases are characterized by the overexpression of zwitterionic amino acid neurotransmitters (ZNTs) into the synaptic cleft, which in abnormal amounts trigger a plethora of processes resulting in the partial impairment or death of nerve cells.[1] Excess secretion of the major excitatory glutamate (Glu) or inhibitory γ-aminobutyric acid (GABA) ZNTs causes an imbalance in the excitation level of the brain, leading to various diseases, such as epileptic seizures that result in the degeneration of neuronal tissue. Thus, decoding the spatio-temporal patterns of brain chemodynamics could imply connection with related diseases. For this reason, ZNTs are recognized as irreplaceable biomarkers for monitoring neuronal activity. Currently, non-invasive imaging techniques based on magnetic resonance (MR), *i.e.* diamagnetic chemical exchange saturation transfer (diaCEST) or ^{13}C MR spectroscopy, are preferably used due to good spatio-temporal resolution and depth of penetration. However, they do not distinguish between intra- and extracellular concentration of ZNTs, and have insufficient chemical resolution and low sensitivity.[2,3] A promising way to address these issues involves the introduction of a paramagnetic sensor capable of altering image contrast upon interaction with the target metabolite.[4] Therefore, the development of MR imaging (MRI) probes responsive to extracellular ZNTs is of emerging importance.

Molecular recognition between magnetic host sensors and guest molecules occurs *via* the formation of a ternary adduct, and is evaluated *via* its binding affinity. In the case of a 'turn-off' response, the interaction of biomarkers with the coordination cage of an MRI probe restricts inner-sphere water accessibility to the paramagnetic center resulting in a signal decrease.[5] So far, the direct sensing of NTs has been approached with two distinct designs, *via* genetically engineered metalloproteins and by small-molecule ditopic paramagnetic probes.[6–8] Although large molecule CAs tailored for monoamine neurotransmitters were shown to be capable of detecting target metabolites in the μM range, further improvement of small-sized probes is imperative due to issues associated with translation into biological systems. In terms of host–guest interaction, the low-molecular-weight sensors are bismacrocyclic Gd(III)-based complexes with a 1,4,7,10-tetraazacyclododecane-1,7-dicarboxylic acid (DO2A) chelator, whose geometry allows for easy access to small anions.[9] In particular, the selectivity of the current sensors is greatly hindered by hydrogencarbonate (HCO_3^-), which binds in a similar fashion as the ZNTs. Owing to high extracellular concentration (~25 mM),[10] small molecular size and consequently low steric hindrances, HCO_3^- predominantly binds to the paramagnetic label, thus preventing selective interaction with ZNTs.[7,8] On the other hand, the advantageous feature of ZNTs is their existence in the form of an ion-pair entity at physiological pH, which opens the possibility of exploiting a ditopic platform to strengthen binding through cooperativity.[11] In accordance with this, different binding modes may unequally affect parameters such as inner-sphere water exchange rate or molecular tumbling (τ_m and τ_R, respectively), which determine both longitudinal (r_1) and transverse (r_2) relaxivities. In turn, the occurrence of non-synchronised changes of r_1 and r_2 would allow for the utilization of the ratiometric r_2/r_1 MRI approach.[12–14]

In order to develop such a sensor, it is necessary to evoke non-synchronized stimuli-induced changes of parameters that determine r_1 and r_2. Therefore, we set out to exploit the cooperative binding potential of a ditopic low-molecular weight Gd-chelate to improve the sensing of ZNTs. The probe design consisted of a bismacrocyclic framework, providing receptor sites to favour cooperative ion-pair binding of ZNTs. The host–guest

MR Neuroimaging Agents, Max Planck Institute for Biological Cybernetics, Tübingen, Germany. E-mail: goran.angelovski@tuebingen.mpg.de

† Electronic supplementary information (ESI) available: Methods, synthetic procedures, and selected spectroscopic and MRI data. See DOI: 10.1039/c9cc06463j

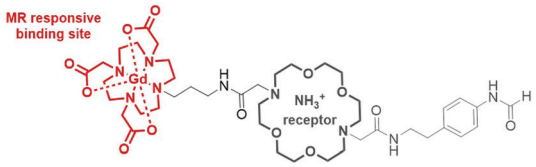

Fig. 1 The chemical structure of the ditopic Gd(III)-chelate, **GdL**.

interactions involve simultaneous coordination of the carboxylate to Gd(III) and multiple hydrogen bonds established between the 18-crown-6 derived moiety (18C6) and the NH_3^+ terminal of ZNTs (Fig. 1).[7,8] The rationale for choosing 1,4,7,10-tetraazacyclododecane-1,4,7-tricarboxylic acid (DO3A) as the MR responsive unit over the coordinatively less saturated DO2A macrocycle is due to its higher selectivity towards carboxylates from ZNTs over HCO_3^-, owing to stronger electronic repulsions from the acetate pendant arms. To reinforce the affinity towards the ammonium cation, we incorporated a formanilide pendant that bears two amide groups, one proximate and one distant to the 18C6 ring-frame, expecting to engage as the H-bond donor and additionally stabilize the binding of the ammonium cation.[15] The role of the flexible amide linker is to preserve the high degree of conformational mobility of the binding sites, providing an adaptable geometry for cooperative binding of the zwitterions (Fig. 2).

The proposed sensor **GdL** was synthesized by bridging two macrocyclic components, followed by complexation with Gd(III) (Scheme 1). The 18C6 fragment **1** was obtained by direct mono-*N* alkylation of the 1,10-diaza-18-crown-6 ether with 2-bromo-*N*-(4-nitrophenethyl)acetamide. Next, the macrocyclic precursors **1** and **2** were covalently linked to form bismacrocyclic derivative **3**. As the preparation of bismacrocycles of this type is often limited by a bridging step, the yield of 62% can be considered as excellent. In the following step, the aromatic nitro group of **3** was subjected to $Pd(OH)_2$/C-catalysed hydrogenation to afford the amine **4**. Simultaneous hydrolysis of the *tert*-butyl esters and conversion of the amine into formamide was conducted in formic acid to obtain the final ligand **L** with a yield of 64%, and a ratio of isomers of 72 : 28.[16] The complexation was performed in water media at neutral pH with $GdCl_3$ to give the corresponding

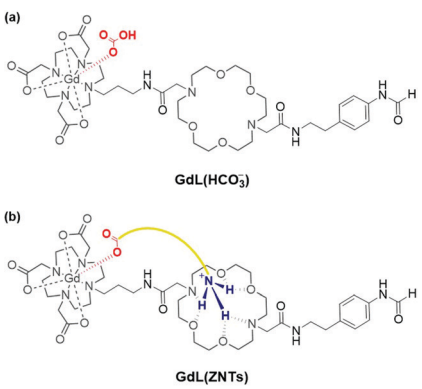

Fig. 2 Binding modes of structurally different guests with **GdL**. (a) Monotopically bound HCO_3^- and (b) ditopically bound ZNT.

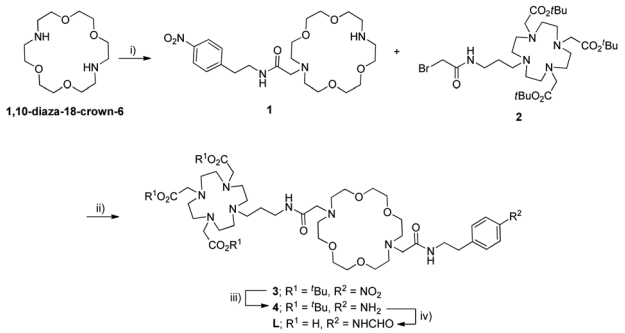

Scheme 1 Synthesis of the crown ether-containing ligand **L**. *Reagents and conditions*: (i) 2-bromo-*N*-(4-nitrophenethyl)acetamide, $NaHCO_3$, MeCN, 45 °C, 52%; (ii) DMF, $NaHCO_3$, RT, 3 days, 62%; (iii) H_2, $Pd(OH)_2$/C (20 wt%), EtOH, 3.1 bar, 84%; (iv) HCOOH, 65 °C, 16 h, 64%.

complex **GdL**. To avoid entrapment of a Gd(III) ion within the 18C6 component, the complexation was performed using a ligand to Gd(III) ratio of 1.0 : 0.8 and the excess of ligand was effectively removed by the HPLC. The absence of free Gd(III) ions was additionally confirmed by the xylenol orange test.

The bulk ^{1}H T_1- and T_2-relaxation time dependencies of **GdL** on the concentration of the ZNTs: Glu, glycine (Gly), GABA, the non-zwitterionic transmitter acetylcholine (ACh) and competitive metabolite HCO_3^- were assessed in relaxometric titrations (Fig. 3). The initial values calculated for r_1 and r_2 were 10.14 and 13.46 mM^{-1} s^{-1}, respectively. The displayed downward trends revealed that **GdL** is ACh-insensitive while HCO_3^- exhibited a comparable drop in r_1 (69%) to the ZNTs that induced changes, with $-\Delta r_1$ ranging from 61 to 69%. However, notably diverse r_2

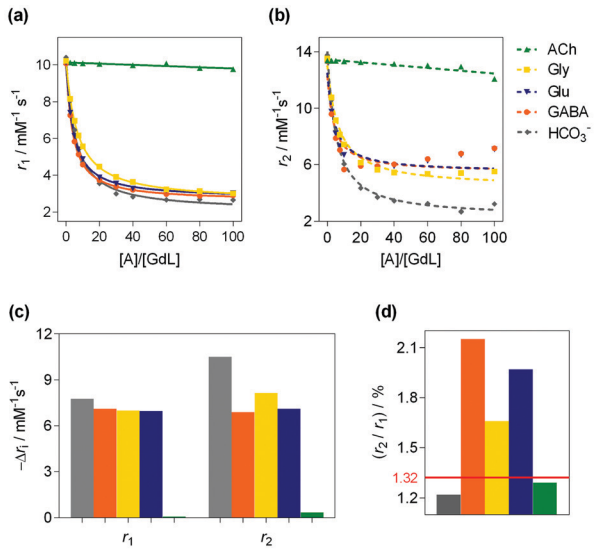

Fig. 3 ^{1}H relaxometric study of **GdL**. (a and b) the experimentally measured (symbols) and fitted data (curves) for (a) r_1 and (b) r_2 relaxivities for **GdL** (2.5 mM) with different analytes (0–100 equiv.) in 50 mM HEPES (pH 7.4, 7.05 T, 298 K). Lines in (a) correspond to the fit described in the ESI,† while the dashed lines in (b) show the mismatch of the experimental to those fitted in the same way, while assuming K_a values obtained from fitting the r_1 data. (c) Decreases in r_1 and r_2 for the host–guest molar ratio of 1 : 60. (d) The corresponding r_2/r_1 ratio.

changes between HCO_3^- and ZNTs were observed. Upon saturation with the guests (60 equiv.), the r_2 of ternary adduct **GdL**-HCO_3^- was 3.69 mM^{-1} s^{-1}, while the values for the -Gly, -Glu and -GABA adducts were 5.64, 5.78 and 5.89 mM^{-1} s^{-1}, respectively.[12] The gathered results are in agreement with the simulations performed for low-molecular-weight Gd(III)-based CAs at high magnetic fields (>1.5 T).[12] Namely, T_1 is relatively constant over a broad range of values for the τ_m and τ_R parameters. On the contrary, for the same parameters, T_2 undergoes a rather drastic change.[12] Hence, the occurrence of non-synchronized changes of T_1 and T_2 within the same MR reporter, opens the possibility to implement a r_2/r_1 ratiometric MRI strategy. When presented as the r_2/r_1 ratio, there is an increase from the initial value of 1.32 for **GdL** to 1.7, 1.9 and 2.1 for Gly, Glu and GABA, respectively. In the case of HCO_3^-, the decrease in r_1 is followed by a proportional decrease in r_2, resulting in insignificant fluctuations for the r_2/r_1 values over the entire titration range.

The binding affinities (K_a) were obtained by fitting the r_1 data to eqn (S2) (ESI†) (Table 1). Comparison of K_a values revealed higher affinities of 116 and 106 M^{-1} for GABA and Glu, respectively, over HCO_3^- and Gly, which were 86 and 64 M^{-1}, respectively. The observed trends suggested greater structural complementarity of the receptor-binding pocket to the long-chain ZNTs, Glu and GABA. Comparing HCO_3^- and Gly, the former binds stronger due to its potential to interact in the bidentate binding mode. The decreased affinity of Gly compared to GABA and Glu is likely due to the absence of cooperative host–guest binding as the carboxylate– amine terminals in GABA and Glu are more suited to the spatial disposition of binding sites within the host. The ambient concentrations of Glu, GABA, Gly and Gln in physiological brain states of ~6 μM, 0.23 μM, 16.7 μM and 1.738 mM, respectively, are still below the detection level of the prepared probe.[17] However, in pathological states the concentrations of ZNTs drastically increase, *e.g.*, in the case of ischemia, Gly reaches a value of 513 μM. Therefore, the affinity constants for **GdL**, which are on the level of ~10 mM, still require slight improvements to allow for the detection of the relevant ZNTs, whose concentrations are closer to low mM values.

The conformational mobility of the binding sites in the host molecule is affected by the interactions with guest molecules. Therefore, to gain insight into the host–guest binding modes, various NMR studies were performed on the diamagnetic yttrium(III) analogue, **YL**.[18] High-resolution ^{1}H NMR spectra were recorded with **YL** in the presence of 20 equiv. of Glu or HCO_3^- (Fig. 4). The resonances of both ternary complexes shifted upfield, with a more pronounced effect for Glu, which suggests its stronger host–guest interaction. Furthermore, splitting

Table 1 The ^{1}H r_1 relaxivity decrease and affinity constants (K_a) of the ternary complexes **GdL**-analyte in 50 mM HEPES (298 K, pH 7.4, 7.05 T)

Analyte	Gly	Glu	GABA	ACh	HCO_3^-
$-\Delta r_1{}^a$ (%)	68	69	71	N/A	75
$K_a{}^b$ (M^{-1})	64	106	116	N/A	86

[a] The values are calculated for the complex to analyte ratio of 1 : 60. [b] Binding affinities were obtained from the fit of r_1 curves to eqn (S2) (ESI).

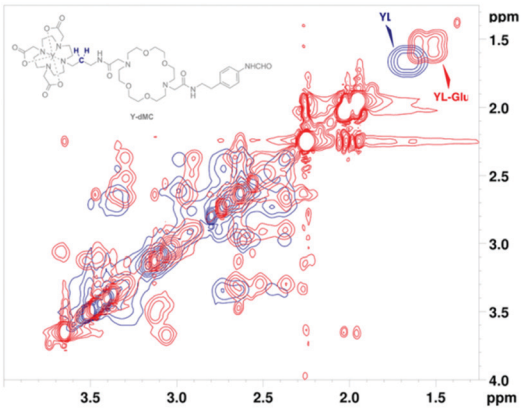

Fig. 4 Overlapped 2D EXSY NMR spectra of **YL** (blue) and **YL**-Glu (red) in D_2O (pD 7.8, 800 MHz).

of the broad signal at 1.69 ppm in ternary adducts, corresponding to the methylene $CH_2\underline{CH_2}CH_2$ of the amide linker that connects the two binding sites, indicated the existence of both bound and non-bound forms. Overall, this revealed host–guest binding with a slow exchange rate and a greater magnitude for **YL-Glu** interactions.

Anion binding to the paramagnetic label coordinated by DO3A-based chelates is well documented, and thus, we focused on investigating interactions that involve the 18C6 binding site. 2D EXSY NMR spectra displayed conformational diversity for the 18C6 moiety within the ternary adducts (Fig. 4 and Fig. S6–S9 in ESI†). The higher density of cross-peaks in **YL-Glu** pointed towards a binding mode that involves multiple interactions between the 18C6 and the ammonium cation. Conversely, the more defined cross-resonances for 18C6 in **YL-HCO_3^-** were assigned to Na^+ inclusion (bicarbonate was added as the monosodium salt). Moreover, no change was observed in the ratio of the isomers in the ^{1}H NMR spectra (see above), which led us to exclude the involvement of the formanilide moiety in binding.

Another parameter sensitive to molecular motions of bound protons is the T_1 relaxation time.[19] Thus, to quantify the observed conformational flipping, we measured T_1 of protons in the $NCH_2\underline{CH_2}O$ groups within the 18C6 fragment and the *meta*-H in the remote pendant (Table S2 and Fig. S10 in ESI†). The acquired T_1 values for the 18C6 moiety in **YL-Glu** and **YL-HCO_3^-** were 692 ms and 651 ms, respectively, whereas the one of binary **YL** was measured to be 628 ms. The elevated T_1 value in the presence of Glu indicated a higher rate of conformational exchange of the 18C6 binding site. This was rationalized as the impact of reversible interactions of multiple hydrogen bonds between NH_3^+ of the zwitterion and free electronic pairs on the heteroatoms in 18C6. Slightly increased mobility of 18C6 in the monotopically bound **YL-HCO_3^-** is likely related to stronger interactions with entrapped Na^+. The identical trend of mobility was observed for the 18C6 pendant, which is in alignment with the higher degree of freedom for linear compounds.

Finally, ^{1}H DOSY NMR measurements provided information on the host–guest association in solution.[20] The obtained self-diffusion constants displayed faster translational motion for the ternary

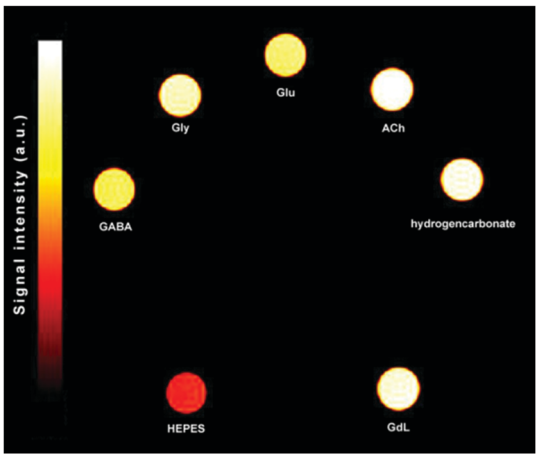

Fig. 5 T_2/T_1w phantom image of **GdL** (1.5 mM) with ZNTs and competitive metabolites in a ratio of 1 : 60 buffered in 50 mM HEPES (298 K, pH 7.4, 7.05 T).

adducts, **YL-Glu** and **YL-HCO_3^-**, compared to the binary **YL** (Fig. S11 and Table S3 in ESI†). The corresponding hydrodynamic radii shrunk from 1.54 nm to 1.29 nm upon moving from the binary complex to the ternary species, suggesting a different spatial arrangement of **YL** prior to its interaction with guests. These values excluded the formation of aggregates or intermolecular self-assembly. The rotational correlation times (τ_R), calculated according to the Stokes–Einstein-Debye model (see ESI†), were identical for the ternary complexes (234 ps), which ruled out molecular tumbling as the explanation for the observed diversity in T_2 trends.[21]

To capitalize on this effect, we tested the selectivity of the **GdL** probe by comparing the signal enhancements of T_1w and T_2w with T_2/T_1w images of MRI tube phantoms in a 7.05 T MRI scanner (Fig. 5 and Fig. S12, S13 and Tables S4, S5 in ESI†). The contrast enhancements were calculated as differences in obtained signal-to-noise ratio (SNR). The T_1w images gave negligible ΔSNRs for Gly, GABA and Glu with respect to the signal enhancement produced by HCO_3^-, which are in the range 1–4%. On the other hand, HCO_3^- caused greater MRI signal alteration in the T_2w images, thus masking the effects of other ZNTs. Specifically, Gly, GABA and Glu only reached 70, 47 and 57% of the signal enhancement observed for HCO_3^-, respectively. In contrast to the results obtained using T_1w and T_2w MRI protocols, the T_2/T_1w phantoms gave more intense signals for Gly, GABA, and Glu compared to HCO_3^- (4, 11 and 10%, respectively). Moreover, HCO_3^- remained completely MR silent with the ΔSNR equal to that of **GdL**. In addition, comparing the greater potential of the T_2/T_1w MRI protocol to the commonly used T_2w analogue to produce images with greater SNR,[14] it should be noted that the effective discrimination of HCO_3^- was successfully achieved under physiologically-relevant conditions.

In summary, we have developed a novel ditopic bismacrocyclic MRI probe with an increased binding affinity towards the major inhibitory (GABA) and excitatory (Glu) neurotransmitters and employed an r_2/r_1 imaging strategy to discriminate from their physiological competitor, HCO_3^-. We demonstrated that the bound guests induced uneven changes of r_1 and r_2 in the supramolecular adducts. Unlike the long-chain ZNTs, the monotopically bound HCO_3^- induced a proportional decrease in both r_1 and r_2, whose ratio remained equal to that of unbound **GdL**. Hence, greater SNR changes were observed for GABA and Glu in MRI phantoms, and were less emphasized for Gly. Overall, these findings establish an efficient strategy to sense polydentate metabolites by employing low-molecular-weight polytopic MR probes. We anticipate that the introduced concept of utilizing a polytopic host with a ratiometric imaging methodology will be beneficial in the future development of MR probes for sensing polycharged guest molecules.

The authors are thankful to Dr Vincent Truffault for measuring NMR spectra and Dr Tanja Savić for recording the MRI phantom images. The financial support of the German Research Foundation (DFG, grant AN 716/7-1) is gratefully acknowledged. Open Access funding provided by the Max Planck Society.

Conflicts of interest

There are no conflicts to declare.

Notes and references

1 J. Lewerenz and P. Maher, *Front. Neurosci.*, 2015, **9**, 469.
2 F. Hyder and D. L. Rothman, *Annu. Rev. Biomed. Eng.*, 2017, **19**, 485–515.
3 K. Cai, M. Haris, A. Singh, F. Kogan, J. H. Greenberg, H. Hariharan, J. A. Detre and R. Reddy, *Nat. Med.*, 2012, **18**, 302–306.
4 G. Angelovski and E. Toth, *Chem. Soc. Rev.*, 2017, **46**, 324–336.
5 S. Aime, M. Botta, J. I. Bruce, V. Mainero, D. Parker and E. Terreno, *Chem. Commun.*, 2001, 115–116.
6 M. G. Shapiro, G. G. Westmeyer, P. A. Romero, J. O. Szablowski, B. Kuster, A. Shah, C. R. Otey, R. Langer, F. H. Arnold and A. Jasanoff, *Nat. Biotechnol.*, 2010, **28**, 264–270.
7 F. Oukhatar, S. Même, W. Même, F. Szeremeta, N. K. Logothetis, G. Angelovski and É. Tóth, *ACS Chem. Neurosci.*, 2015, **6**, 219–225.
8 F. Oukhatar, H. Meudal, C. Landon, N. K. Logothetis, C. Platas-Iglesias, G. Angelovski and É. Tóth, *Chem. – Eur. J.*, 2015, **21**, 11226–11237.
9 S. Aime, A. Barge, M. Botta, J. A. K. Howard, R. Kataky, M. P. Lowe, J. M. Moloney, D. Parker and A. S. de Sousa, *Chem. Commun.*, 1999, 1047–1048.
10 M. Chesler, J. C. T. Chen and R. P. Kraig, *J. Neurosci. Methods*, 1994, **53**, 129–136.
11 A. Galan, D. Andreu, A. M. Echavarren, P. Prados and J. Demendoza, *J. Am. Chem. Soc.*, 1992, **114**, 1511–1512.
12 P. Caravan, C. T. Farrar, L. Frullano and R. Uppal, *Contrast Media Mol. Imaging*, 2009, **4**, 89–100.
13 S. Okada, S. Mizukami, T. Sakata, Y. Matsumura, Y. Yoshioka and K. Kikuchi, *Adv. Mater.*, 2014, **26**, 2989–2992.
14 S. Gündüz, T. Savić, R. Pohmann, N. K. Logothetis, K. Scheffler and G. Angelovski, *ACS Sens.*, 2016, **1**, 483–487.
15 S. Blanco, P. Pinacho and J. C. Lopez, *Angew. Chem., Int. Ed.*, 2016, **55**, 9331–9335.
16 A. J. R. Bourn, E. W. Randall and D. G. Gillies, *Tetrahedron*, 1964, **20**, 1811–1818.
17 P. J. Hutchinson, M. T. O'Connell, P. G. Al-Rawi, C. R. Kett-White, A. K. Gupta, L. B. Maskell, J. D. Pickard and P. J. Kirkpatrick, *J. Neurol. Neurosurg. Psychiatry*, 2002, **72**, 99–105.
18 M. Ciardi, A. Galan and P. Ballester, *J. Am. Chem. Soc.*, 2015, **137**, 2047–2055.
19 E. J. Bang, J. W. Jung, W. J. Lee, D. W. Lee and W. T. Lee, *J. Chem. Soc., Perkin Trans. 2*, 2001, 1685–1692.
20 G. Pages, V. Gilard, R. Martino and M. Malet-Martino, *Analyst*, 2017, **142**, 3771–3796.
21 M. Roos, M. Ott, M. Hofmann, S. Link, E. Rossler, J. Balbach, A. Krushelnitsky and K. Saalwachter, *J. Am. Chem. Soc.*, 2016, **138**, 10365–10372.